Journal of Industrial and Management Optimization

JIMO, 22(3): 1361−1393.
DOI: 10.3934/jimo.2026050
Received: 23 July 2025
Revised: 25 January 2026
Accepted: 30 January 2026
Published: 11 February 2026

https://www.aimspress.com/journal/jimo

Research article

Research on IPSO-SVM silicon material supply and demand early warning method based on supply chain perspective

Dudu Guo[1,2,*], Xue Zhang[3], Peifan Jiang[3], Xiaojiang Zhang[4] and Jinquan Zhang[5]

[1] Transportation Engineering, Xinjiang University, Urumqi 830017, China
[2] Xinjiang Key Laboratory of Green Construction and Smart Traffic Control of Transportation Infrastructure, Xinjiang University, Urumqi 830017, China
[3] School of Business, Xinjiang University, Urumqi 830017, China
[4] Xinjiang Xinte Energy Logistics Co., Urumqi 830017, China
[5] Xinjiang Hualing Logistics & Distribution Co., Urumqi 830017, China

* **Correspondence:** Email: guodd@xju.edu.cn.

Abstract: With the rapid growth of the photovoltaic industry, the instability of the silicon market has led to an imbalance in silicon supply and demand. To address this problem, this paper proposes an early-warning method for silicon supply/demand based on the improved particle swarm algorithm optimized support vector machine (IPSO-SVM). First, based on a supply chain perspective from the supply and demand sides using time-difference correlation analysis, the impact of silicon supply/demand balance on five warning indicators was determined, as well as a benchmark indicator of seven warning levels and warning thresholds. The silicon supply/demand warning model, based on the IPSO-SVM, suffers from the drawbacks of the PSO algorithm, including a tendency to converge to local optima and slow convergence. To address these limitations, a combined optimization strategy was applied to the PSO and integrated within the IPSO-SVM model to achieve self-adaptive parameter tuning. Warning indicators were used as model inputs, and the warning level of the benchmark indicators served as the model output, enabling the model to predict the category of the warning level. Finally, this study introduces an enterprise X dataset for validation. The results show that, compared with a PSO-SVM model with single-strategy optimization, IPSO-SVM achieves an average accuracy improvement of 3.51%. Compared with the standard PSO-SVM model, IPSO-SVM achieves an average accuracy improvement of 4.35%. Moreover, relative to SVM classification models optimized by various other algorithms, IPSO-SVM attains an average accuracy gain of 12.28%, with a notable

improvement of 7.45% for the minority class, thereby significantly enhancing the overall performance of the classification model.

Keywords: supply chain; supply and demand warning; particle swarm algorithm; support vector machine
Mathematics Subject Classification: 2020 *Mathematics Subject Classification.* Primary: 68T01, 90B20; Secondary: 65K05

1. Introduction

In recent years, the photovoltaic (PV) industry has experienced rapid technological innovation, significant cost reductions, and the continuous expansion of application areas, demonstrating vigorous global growth. Concurrently, faced with economic development models characterized by high consumption and high pollution, countries worldwide are actively seeking green, low-carbon energy alternatives. Consequently, the economic advantages of solar energy are becoming increasingly apparent compared to traditional energy sources such as coal. Currently, more than 40 countries around the world have introduced policies to support photovoltaic power generation, and this number is rising year by year, signaling a rapid, multi-fold expansion of the global PV power generation market [1]. As the foundational material of the PV industry, silicon-based materials have seen continuous scaling of production, declining costs, and improving product quality. The polysilicon industry itself is undergoing a profound transformation, marked by clear trends of internal structural change [2].

The growing demand for silicon-based materials, as the essential raw input for PV manufacturing, has attracted numerous enterprises to increase production and investment. However, this surge in market demand may lead to an overshoot, potentially causing a significant imbalance between the supply and demand of silicon materials [3]. Such an imbalance poses substantial risks to industry stability. Therefore, establishing an early-warning mechanism for supply/demand imbalances is crucial, enabling enterprises to make timely adjustments.

In production planning, enterprises often aim to maximize output based on sales, maintaining inventory levels sufficient to meet basic order requirements. The goal is to maintain a dynamic balance between supply and demand, where the supply/demand ratio fluctuates within an acceptable range rather than statically equaling 1. The silicon material market has been shaped in recent years by supportive PV policies and external shocks, leaving it susceptible to sudden demand surges or oversupply. An effective early-warning system is essential to help enterprises anticipate and mitigate the impacts of these extremes.

In summary, the main contributions of this paper include the following three points:

(1) Factors affecting the silicon supply/demand ratio are analyzed, and their correlation is quantified from a supply chain perspective. Using time-lag correlation analysis, we quantify the relationship between these factors and the supply/demand ratio, enhancing the objectivity and validity of subsequent warning level classification and prediction.

(2) An early-warning model based on an improved particle swarm algorithm optimized support vector machine (IPSO-SVM) is proposed. To overcome the limitation of the traditional particle swarm optimization (PSO) algorithm easily falling into local optima, key parameters are adaptively improved, strengthening both global search and local development capabilities. The key improvements are theoretically grounded in stability analysis, ensuring convergence and practical acceleration while

maintaining low computational complexity. To enhance the classification accuracy of support vector machine (SVM) for small-sample data, the improved PSO is used to optimize SVM parameters, improving model training convergence speed and performance.

(3) In-depth experimental evaluation demonstrates that the proposed method achieves better classification performance compared to traditional models, is effective for small-sample category prediction, and handles imbalanced categories well.

The remainder of the paper is organized as follows: Section 2 provides a literature review of related work. Section 3 details the methodology of our proposed silicon supply/demand early-warning method. Section 4 provides a detailed introduction to the optimization research of the support vector machine model based on the IPSO algorithm. Section 5 presents the case study and results analysis. Finally, Section 6 summarizes the paper and outlines future research directions.

2. Literature review

In recent years, research on supply and demand early warning has mainly focused on identifying and predicting tensions caused by imbalances in the supply and demand of key resources. Existing research typically follows two paradigms: one is to conduct early warning first, followed by prediction; the other is to conduct prediction first, followed by triggering early warning. In these paradigms, most methods can be divided into two categories: prediction-oriented methods, which focus on estimating the fluctuation of demand or supply quantity, and classification-oriented methods, which are used to identify anomalies, failures, or sudden structural changes in the system.

Existing research specifically targeting early-warning systems for silicon material supply/demand imbalances is limited. Some scholars have approached the issue from the demand side; for instance, X. Hu et al. [4] proposed an interpretable multi-prediction model for PV solar power forecasting, which aims to prepare supply by predicting demand. Other studies on bulk commodities like coal offer relevant insights; Y. Feng et al. [5] developed a mechanism to predict coal supply and demand, using the ratio of inventory to consumption to determine market balance.

However, most existing early-warning studies focus on specific resources like electricity, typically involving separate predictions for supply and demand before assessing imbalance. Few adopt a supply chain perspective. While scholars such as Y. Yang [6], L. Tao [7], and J. Wang [8] have studied recovery strategies for supply-demand imbalances within supply chains, their work often focuses on post-disruption responses. The unique characteristics of silicon production—featuring long capacity cycles and low-capacity elasticity—make a proactive early-warning system particularly critical. Long capacity cycles mean that once a shortage occurs, it takes considerable time for new capacity to come online; low elasticity means outputs cannot be quickly increased through measures like overtime. Furthermore, silicon prices are highly susceptible to external policies and market demand fluctuations. Therefore, by combining the capacity characteristics of silicon with the development traits of the PV industry, enterprises require a supply/demand early-warning mechanism based on a comprehensive understanding of their position within the silicon material supply chain. This paper addresses this need by proposing an early-warning method for silicon materials from a supply chain perspective.

Prediction-oriented studies in supply/demand early warning primarily employ time-series models, machine learning, and hybrid frameworks to capture demand volatility and supply uncertainties, while classification-based approaches focus on anomaly detection to provide timely alerts. Although both directions advance early-warning theory, most remain limited to resource-level analyses without fully addressing supply chain interdependencies. From a supply chain management perspective, early-

warning systems are increasingly regarded as essential for risk monitoring and resilience enhancement. For instance, H. Tang et al. [9] combined demand forecasting with supply chain optimization under uncertainty. Recent work further proposes dynamic, data-driven frameworks that merge statistical learning, probabilistic modeling, and optimization, extending early-warning applications to supplier risk, demand fluctuation, and disruption forecasting. Nonetheless, most studies emphasize predictive accuracy or classification performance in isolation, with limited integration into supply chain operations.

Accordingly, this study contributes by bridging predictive analytics and early-warning mechanisms from a supply chain perspective. Through an integrated framework that couples forecasting, anomaly detection, and supply chain dynamics, it aims to enhance both interpretability and practical effectiveness in supply/demand risk management.

2.1. Objects of supply/demand early warning

Regarding supply/demand early warning, many scholars have evaluated early warning for scarce or commonly used resources in a certain region, such as water resources, mainly designing and studying the early-warning mechanism and process. H. Tang et al. [9] used system dynamics methods to construct a simulation model of an early-warning system for urban development and water resource demand in the oasis of arid zones, carrying out a multi-scenario simulation. Q. Li et al. [10] assessed water resource supply and demand on a regional, short-term scale in the context of early warning, proposing an early-warning index system of water resource supply/demand and determining criteria for different early-warning levels. Some researchers have also considered early-warning systems for the supply/demand of food and agricultural products. Y. Zheng, J. Ma [11] used the smoothness test, Granger test, and regression analysis to study the association between short-term supply/demand imbalance and price fluctuation of agricultural products, classifying the early-warning level according to the difference between the supply and the demand. H. Lu et al. [12] used the pooled empirical modal decomposition (EEMD) model to analyze time-series data of the price of the Chinese wholesale potato market and conduct early warnings on the price. W. Yang et al. [13] analyzed the time series data of potato wholesale market prices in China using the ensemble empirical modal decomposition (EEMD) model to forecast prices. Research on early warning regarding certain scarce and commonly used resources is also noteworthy, particularly using prediction methods. J. Sun et al. [14] conducted non-equilibrium analyses on the effective supply and demand of China's rare earth market and established hyperbolic aggregation equations. Y. Zhao et al. [15] combined adaptive Y. Li et al. [16] to establish a patent early-warning evaluation program, adopting patent analysis and expert evaluation methods to carry out early warnings. S. An et al. [17] proposed an anisotropic network model that identifies key changes based on the structure of the network associations that represent the dynamic process of time-series early warning. K. Zhou et al. [18] used the gated recurrent unit and long short-term memory model to forecast power generation and consumption. Based on the prediction results, they proposed an energy supply/demand interaction model that assists the energy system in achieving dynamic matching between energy supply and demand.

In summary, prior research has predominantly focused on early-warning systems for specific resources, such as water, food, agricultural products, rare earths, patents, and energy, employing methods that range from indicator system construction to econometric modeling and machine learning integration. While these studies offer important insights, they underscore the necessity of developing more comprehensive and adaptable frameworks capable of addressing heterogeneous resource types and rapidly evolving supply/demand dynamics.

2.2. Methods of supply/demand early warning

Regarding the early warning of supply and demand, many scholars have achieved early warning by forecasting supply and demand. For example, X. Yao et al. [19] proposed a new dynamic seasonal gray model based on PSO-SVR to predict the production and consumption of electricity, considering that data on both supply and demand of electricity undergo obvious seasonal fluctuations. M. Pinhão et al. [20] attempted to predict the dynamics behind the tariffs by market curve modeling and forecasting. G. Lin et al. [21] proposed a hierarchical design of an energy supply/demand forecasting system based on the web crawler and grey dynamic model GM (1,1), obtaining higher prediction accuracy. H. Song et al. [22] proposed a new quantitative prediction model for pork supply that combines a supply model with a consumption model, which combines production and imports/exports.

Price is also believed to be an important factor influencing the fluctuation of supply and demand of a certain good; therefore, researchers undergo forecasting of the price or market economic fluctuations to evaluate the future supply/demand situation. For example, Y. Chen et al. [23] used multi-objective optimization with life cycle assessment (LCA) to evaluate an integrated energy system (IES) — addressing energy, environmental, and cost challenges, with cost-saving insights and price sensitivity.

Some scholars also considered the impact of emergencies and natural disasters on the supply/demand relationship. Z. Shi et al. [24] simulated and analyzed how natural disasters negatively affect food production and consumption using China's agricultural industry model. They proposed paying attention to the international food supply chain, strengthening monitoring and early warning, and continuously improving food security risk management and control capabilities. X. Zhao et al. [25] used a linear weighting method and artificial neural network (ANN) to construct a joint early-warning system for predicting forestry supply and demand security.

Some scholars used the classification model to classify the supply or demand and level of vigilance. For example, H. Cai et al. [26] classified the electricity consumption level for energy supply and demand of residential buildings. The particle swarm optimization K-means algorithm was applied to the cluster analysis, and the electricity consumption levels were divided by the cluster centers; subsequently, an efficient classification model with support vector machine as the basic optimization framework was proposed, and its feasibility was verified. Z. Li et al. [27] proposed an approach to optimize the parameters of the support vector machine (SVM) by using the improved artificial hummingbird algorithm (IAHA) and a coal mine environmental safety warning model that combines various environmental parameters to classify its safety level.

Overall, current early-warning research primarily adopts prediction-driven models, complemented by classification techniques. These methods improve forecasting accuracy but reveal the necessity for more resilient frameworks that address complex interactions and systemic uncertainties in supply/demand dynamics.

2.3. Application of the PSO-SVM model

Parameter setting by traditional support vector machines lack a certain degree of flexibility, where samples lack adaptability. Therefore, algorithms are often used to find optimal parameter values of the support vector machine; the particle swarm algorithm (PSO) is the most commonly used to optimize the support vector machine (SVM) to construct a classification model for prediction and warning, by finding the optimal solution of the parameters of the SVM to improve the prediction effect of the model. E. Bonah et al. [28] proposed a model using heuristic algorithms to optimize the modeling parameters c and g of the SVM for the classification and differentiation of bacterial foodborne

pathogens. Y. Sun [29], Q. Song [30], L. Tian [31], Y. Liang [32] used PSO algorithms to optimize the parameters of SVM and constructed PSO-SVM models with strong generalization to classify and predict different research objects. Other scholars improved the PSO-SVM model by combining the characteristics of the research objects to improve the performance of the PSO-SVM model in classification prediction. M. Li et al. [33] introduced the PCA for dimensionality reduction and then selected optimal parameters through the PSO optimization algorithm to construct the prediction model of PCA-PSO-SVM. H. Ren et al. [34] used the optimization of the least squares support vector machine (LSSVM) model parameters by PSO to improve the fit between the model and the research object. A. Qin et al. [35] proposed a relatively new hybrid intelligent fault classification by integrating multiple dimensionless parameters, Fisher's criterion, and PSO-SVM. Y. Wei et al. [36] proposed an intelligent fault diagnosis algorithm for rotating machinery based on intrinsic characteristic scale decomposition (ICD), generalized composite multiscale fuzzy entropy (GCMFE), Laplace scoring (LS), and particle swarm optimization-based support vector machine (PSO-SVM). M. Li et al. [37] presented an intelligent fault classification algorithm for rotating machinery based on a novel noise suppression framework with improved PSO-SVM. C. Xu et al. [38] proposed a method for detecting and recognizing surface defects of lithium battery pole pieces based on multi-feature fusion and PSO-SVM.

As shown, most research on supply/demand early warning focuses on the state of macro resources, and early-warning methods are closely linked to prediction. These methods use intelligent algorithms trained on historical data to forecast future supply and demand to achieve early warning. Most studies consider macroscopic objects and contexts—typically, common scarce resources. In contrast, fewer studies exist on micro-level supply/demand early warning for individual enterprises. There is an increased number of studies on the establishment of early-warning indicator systems and the construction of an early-warning mechanism, but there is a lack of literature regarding the detailed introduction of early-warning thresholds. Still, the design of macro-level supply/demand early-warning mechanisms in previous studies provides a theoretical basis for subsequent micro-level early-warning within enterprises. Moreover, macro-level early-warning indicators can serve as external factors influencing the internal supply of the enterprise.

Scholars have addressed the problem of supply/demand imbalance from two perspectives. On one hand, some focus on predicting supply and demand and then conducting comparisons. They consider the most significant factors affecting supply and demand, such as prices and the economic situation. On the other hand, a few scholars focus on fluctuations in supply and demand. They optimize SVMs using PSO for classification, which is a more mature research approach. Many scholars have also explored using adaptive strategies to optimize the parameters of the PSO. However, most studies focus on improving a single parameter. This approach is more suitable for large sample data, but the prediction accuracy for small samples has not yet reached its potential.

This paper proposes an improved particle swarm algorithm optimized support vector machine based on the supply chain perspective for a silicon supply/demand early-warning method. First, from the perspective of the supply chain, the supply/demand ratio of silicon materials is influenced by multiple factors in the external market and internal production. Time-difference correlation analysis is used to assess the relationship between these factors and the supply/demand ratio. The correlated factors are then used as early-warning indicators to jointly determine the warning levels for silicon supply/demand ratio. Next, the traditional particle swarm algorithm is improved by combining three parameter optimization strategies, and the parameters of the SVM are optimized by such improved particle swarm algorithm, to predict the warning levels for silicon material supply/demand ratio.

In summary, although prior studies have verified the effectiveness of PSO-SVM and its variants

in improving classification and prediction performance, most research remains concentrated on macro-level resources and lacks targeted applications at the enterprise scale. This underscores the imperative to develop more sophisticated models that incorporate adaptive optimization strategies, thereby enabling more precise and context-specific early warning of micro-level supply/demand dynamics.

3. Methods

3.1. Introduction of the problem

As different silicon materials play different roles in the PV industry, different silicon materials are in different positions in the silicon supply chain, and their supply and demand status is also affected by different factors. However, they are all affected by upstream supply and downstream demand, as well as their price dynamics and changes. Therefore, the early-warning problem of supply and demand of silicon materials needs to be viewed from the perspective of the supply chain.

The usual indicator for determining supply and demand is the supply/demand ratio, which determines whether there is under- or oversupply. The formula for the supply/demand ratio (SDR_i) is as follows:

$$SDR_i = \frac{S_i}{D_i} \times 100\% \tag{1}$$

Where S_i is the supply in the period i, and D_i is the demand in the period i. When SDR_i is equal to 1, there is absolute equilibrium. However, in real-life enterprises, the supply/demand ratio shows dynamic fluctuations, making it extremely rare to have a ratio of 1. Therefore, a more detailed classification of the state of the supply/demand ratio using warning levels is necessary.

Early warning can be distinguished between 1) forecasting before warning, in which there is a two-way forecasting of supply and demand, and then forecast results are transformed into supply/demand ratios before judging the early warning, and 2) forewarning before forecasting, where historical supply and demand data are transformed into supply/demand ratios, which are then split into warning levels and thresholds that are used to forecast warning levels. Considering certain limitations in judging the supply and demand status of a certain resource using the supply/demand ratio, this paper adopts the latter idea of early warning and considers factors that correlate with this ratio.

This study investigates the factors influencing the balance of silicon material supply and demand from a supply chain perspective. A time-difference correlation analysis is applied to identify the relationship between these factors and the supply/demand ratio, which is further adopted as a warning indicator. To enhance prediction accuracy, the traditional particle swarm optimization algorithm is improved through three parameter optimization strategies, and the optimized algorithm is used to tune the parameters of a support vector machine. On this basis, an early-warning method for silicon material supply and demand is developed, integrating supply chain analysis with the improved particle swarm optimization–support vector machine model.

3.2. Early-warning indicator analysis of silicon material supply and demand based on a supply chain perspective

3.2.1. Analysis of factors affecting supply/demand balance of silicon materials based on a supply chain perspective

The supply/demand ratio of silicon is influenced by upstream supply, downstream demand, and substitutable products. This study takes polysilicon as an example. Its upstream raw material is industrial silicon, and its downstream product is silicon wafers. Based on its position in the supply chain, the supply and demand of polysilicon are analyzed within and outside the enterprise. The key factors affecting the supply/demand ratio are identified. Figure 1 illustrates polysilicon from both upstream and downstream perspectives.

In the external market environment, several factors influence the supply/demand ratio of polysilicon. First, changes in the price of its upstream raw material (industrial silicon) affect the order quantity of polysilicon. Second, the price of its downstream product (silicon wafers) directly influences the demand for polysilicon. In addition, polysilicon faces competition from substitutes such as monocrystalline silicon. Price fluctuations of these substitutes also impact downstream demand for polysilicon. Therefore, this paper selects several key factors to study the supply/demand balance of polysilicon. These include the price of industrial silicon, the order quantity of industrial silicon, and the consumption of industrial silicon, as well as the price of silicon wafers, the price of substitutes, and the price of polysilicon itself.

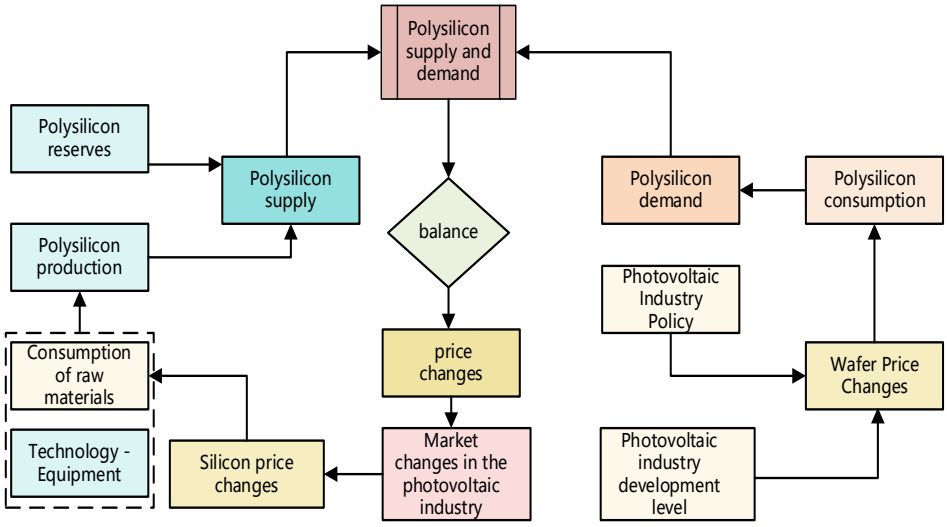

Figure 1. Analysis of polysilicon supply/demand relationship.

3.2.2. Selection of early-warning indicators

In this paper, time-difference correlation analysis is used to analyze the degree of correlation between various influencing factors and the silicon supply/demand ratio, to determine early-warning indicators. Time-difference correlation analysis uses correlation coefficients to verify the relationship between the economic time series (consistent or lagging). The calculation steps are as follows:

(1) Calculate the time-difference correlation coefficient

The time-difference correlation coefficient is computed by selecting a key economic indicator

that sensitively reflects current economic activity as the benchmark indicator. The chosen indicator is then lagged or led by several periods to compute the corresponding correlation coefficients.

Let $y = (y_1, y_2, \ldots, y_n)$ be the warning indicator, $x = (x_1, x_2, \ldots, x_n)$ be the early-warning indicator, and r_l the time-difference correlation coefficient.

$$r_l = \frac{\sum_{t=t'}^{n_l}(x_{t+l} - \bar{x})(y_t - \bar{y})}{\sqrt{\sum_{t=t'}^{n_l}(x_{t+l} - \bar{x})^2 \sum_{t=t'}^{n_l}(y_t - \bar{y})^2}} \tag{2}$$

$$l = 0, \pm 1, \pm 2, \ldots, \pm L \textit{(Math.) genust}' = \begin{Bmatrix} 1 & l \geq 0 \\ 1 - l & l < 0 \end{Bmatrix}$$

Where l denotes the overrun or lag period and is known as the time difference or delay number (l = 0 for synchronization, l < 0 for overrun, l > 0 for lag). n is the number of data points. l denotes the maximum delay number, where values different than l are taken to represent different time differences. The time-difference correlation coefficients are calculated taking the largest absolute value as the time-difference correlation coefficient.

(2) Select early-warning indicators

First, according to the general classification of correlation coefficients in Table 1, influencing factors with very weak correlation or no correlation (i.e., correlation coefficients at [0.0,0.2) are excluded. The remaining factors are defined as the warning indicators, and the ratio of supply and demand of silicon materials is determined as the benchmark indicator.

Table 1. Classification correlation coefficients.

Form	Extremely weak correlation	Weak correlation	Moderately relevant correlation	Strong correlation	Highly relevant correlation
r_l	[0,0.2)	[0.2,0.4)	[0.4,0.6)	[0.6,0.8)	[0.8,1.0]

The selection of early-warning indicators should follow certain principles. In addition to accessibility and quantifiability, the principles of scientific, representativeness, and relevance must be considered. Therefore, it is necessary to test the correlation between warning indicators and benchmark indicators. This ensures that the selected indicators can scientifically and reasonably reflect changes in the benchmark indicators. Grey relational analysis (GRA) is an important method in grey systems theory for measuring the degree of association between factors. It is based on the degree of similarity or dissimilarity of trends between factors and determines the degree of association by comparing the degree of geometric similarity of the data series of each factor. It can indicate the degree of correlation between each indicator and the ratio of silicon supply and demand through the degree of correlation, and once again verify the validity of the selected indicators.

3.2.3. Determination of early-warning levels

This paper applies the Six Sigma principle to determine the warning levels for the silicon market supply/demand situation. The Six Sigma principle is adopted due to its proven effectiveness in quality control and process management for identifying statistically significant deviations from the mean [11]. Based on this analysis, the warning level and threshold range of each indicator are determined. Specifically, warning thresholds are established at ±1.5σ (yellow alert), ±3σ (orange alert), and beyond ±3σ (red alert), corresponding to expected probabilities of deviation in stable processes. Then, the

weights obtained from the time-difference correlation analysis of each indicator are incorporated. Finally, the comprehensive warning level and threshold range for the baseline indicator—the silicon supply/demand ratio—are established.

(1) Determination of warning levels for warning indicators

Using the Six Sigma principle $\mu \pm 3\sigma$, i.e., $(-\infty, \mu - 3\sigma)$, $[\mu - 3\sigma, \mu - 2\sigma)$, $[\mu - 2\sigma, \mu - \sigma)$, $[\mu - \sigma, \mu + \sigma)$, $[\mu + \sigma, \mu + 2\sigma)$, $[\mu + 2\sigma, \mu + 3\sigma)$, $[\mu + 3\sigma, +\infty)$ indicates the fluctuation of the rate of change of the supply/demand ratio of silicon materials in the external objective market. Next, the fluctuation of the supply/demand ratio in the domestic market is observed. Based on historical data, the fluctuation range within each threshold is determined. Finally, the fluctuation ratio is compared with the Six Sigma level table. This comparison defines the warning threshold range of each indicator and its corresponding level.

(2) Determination of early-warning levels for baseline indicators

To determine the warning level and threshold value of the benchmark indicator (silicon supply/demand ratio) based on the warning level and threshold value of each warning indicator, first we calculate the weight of the correlation coefficient of the time difference between each warning indicator and the benchmark indicator (silicon supply/demand ratio ω_i). Then, we determine the warning level and threshold value of the benchmark indicator based on the warning levels and thresholds of each warning indicator. First, we compute the weight of the correlation coefficient between the time-difference of each warning indicator and the benchmark indicator, denoted as ω_i, using the following formula:

$$\omega_i = \frac{|r_i|}{\sum_1^n |r_i|} \tag{3}$$

Where r_i denotes the time-difference correlation coefficient between each warning indicator and the benchmark indicator; $\omega_i > 0$, and $\sum_1^n |\omega_i| = 1$, i=1,2, 3..., n (n is the number of warning indicators).

For the different warning levels of early-warning indicators to design the score and set the baseline of the early-warning index (generally for the normal state of the early-warning index), the historical moment of each period of the early-warning index Z_j is calculated as follows:

$$Z_j = \frac{\sum_{j=1}^n ()}{d \times \omega_i \times W_{j+l} z} \tag{4}$$

Where Z_j denotes the current warning index, ω_i denotes the weight of the correlation coefficient of different warning indicators, W_{j+l} denotes the score of warning indicators for the lead or lag period, l denotes the lead or lag period, d is the score of the normal state level, and z is the warning index of normal state level.

According to the calculated historical moment early-warning index, the mean and standard deviation of the early-warning index are computed to determine its warning level and threshold. Therefore, the level and threshold of the early-warning index, weighted by the correlation coefficient of the time difference for each warning index, correspond to the early-warning level and threshold of the current period's supply/demand ratio change rate for silicon materials.

3.3. Support vector machines

3.3.1. Overview of support vector machines

SVMs are a class of generalized linear classifiers for binary classification of data by supervised learning, whose decision boundary is the maximum-margin hyperplane solved for the learning samples. The decision boundary is the maximum-margin hyperplane solved for the learning samples, and the optimal hyperplane equation is $f(x) = \omega x + b$.

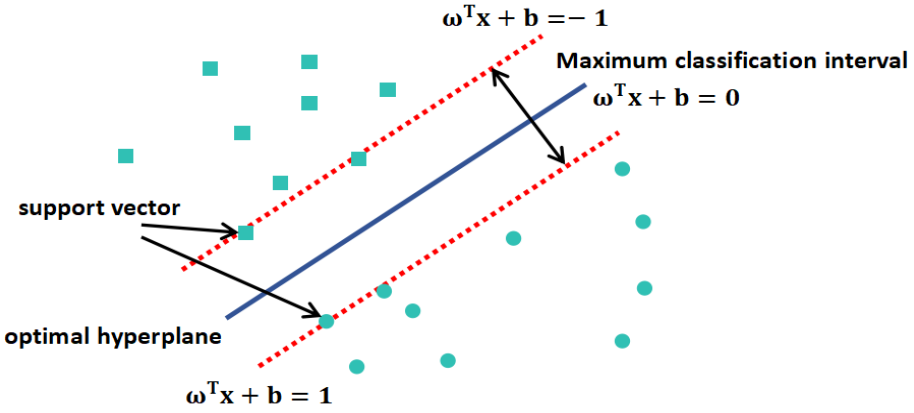

Figure 2. Support vector machine overview diagram.

Since SVM uses the structural risk minimization criterion to train the classifier, it can better deal with the problems of nonlinearity of sample features and high dimensionality, making it capable of classification. In practical applications, the performance of SVM mainly relies on the selection of the penalty factor c and the parameter g of the kernel function [39].

3.3.2. Parameter optimization

The hyperparameters in SVM have a significant impact on classification performance. When solving real classification problems, these hyperparameters need to be adjusted. Key hyperparameters to optimize include the penalty factor c and the kernel parameter g.

(1) Penalty factor c: a penalty imposed on misclassified samples that serves to limit the number of deviation points. As the degree of control over the deviation points in the space becomes larger, the value of c will be larger accordingly. The penalty parameter c can balance the confidence range and empirical risk in certain feature spaces to achieve the best generalization ability of the model.

(2) Nuclear parameters: The kernel function maps the sample dataset from a low-dimensional space to a high-dimensional space. By calculating the function value in the low-dimensional space, the inner product of the samples in the mapped high-dimensional space can be obtained without explicit transformation. This makes it possible to find the optimal classification surface. Therefore, the choice of kernel function is crucial for constructing nonlinear SVMs. Currently, the kernel functions shown in Table 2 are the most frequently used when solving classification problems with SVMs.

For different classification problems, the choice of kernel function affects the final model's performance to varying degrees. For example, the linear kernel function is simple but cannot handle nonlinear problems. In the RBF kernel, the parameters determine the complexity of how samples are

mapped from the low-dimensional space to the high-dimensional space. The sigmoid kernel has two parameters that need to be set, which makes the optimization process more computationally intensive.

Table 2. Common kernel functions.

Name	Analytic formula	Note
Linear kernel	$K(x_i, x_j) = x_i^T x_j$	The inner product of the original space
Polynomial kernel	$K(x_i, x_j) = (x_i^T x_j + 1)^d$	$d \geq 1$ is the number of polynomials
Gaussian kernel (RBF kernel)	$K(x_i, x_j) = \exp(-\frac{\|x_i - x_j\|^2}{2\sigma^2})$	$\sigma > 0$ is the bandwidth of the Gaussian kernel
Laplacian kernel	$K(x_i, x_j) = \exp(-\frac{\|x_i - x_j\|}{\sigma})$	
Sigmoid kernel	$K(x_i, x_j) = \tanh(\beta x_I^T x_j + \theta)$	tanh is a hyperbolic tangent function, $\beta > 0, \theta > 0$

3.4. Particle swarm algorithm

Particle swarm algorithm [full name, particle swarm optimization (PSO)] is a search algorithm based on group collaboration developed by simulating the foraging behavior of bird flocks. The PSO belongs to the heuristic algorithm, also called the intelligent optimization algorithm, and its basic idea is to find the optimal solution through collaboration and information sharing among individuals in the group [40].

In the traditional SVM classification model, the selection of the penalty factor c and the kernel function parameter g has a more significant impact on the accuracy of SVM classification results. However, traditional SVM models usually set parameter values manually. This approach lacks objectivity and cannot adapt to different sample data. To address this issue, an appropriate algorithm is needed to find the optimal SVM parameters. In this paper, an improved PSO algorithm is used to determine the optimal values of c and g for SVM.

4. Optimization of the SVM model based on an improved PSO

In this paper, we first use the time-difference correlation analysis method to identify the warning indicators affecting the balance of silicon material supply and demand. We then determine the alertness levels and warning thresholds for each indicator and for the benchmark indicator—the silicon material supply/demand ratio. The resulting data samples are input into the classification model of the improved particle swarm optimization (IPSO)–optimized support vector machine. In this model, the warning indicators serve as inputs, and the alertness of the benchmark indicator serves as the output. Since the sample data in this paper is small, traditional PSO parameters, which are mostly static and manually set, lack adaptability. To improve the algorithm's adaptability to sample characteristics, a combinatorial strategy is used to make key parameters self-adaptive. The IPSO is then applied to optimize the parameters of the support vector machine. This enhances the accuracy of the overall warning model. Figure 3 shows the flowchart of the early-warning model based on IPSO-SVM.

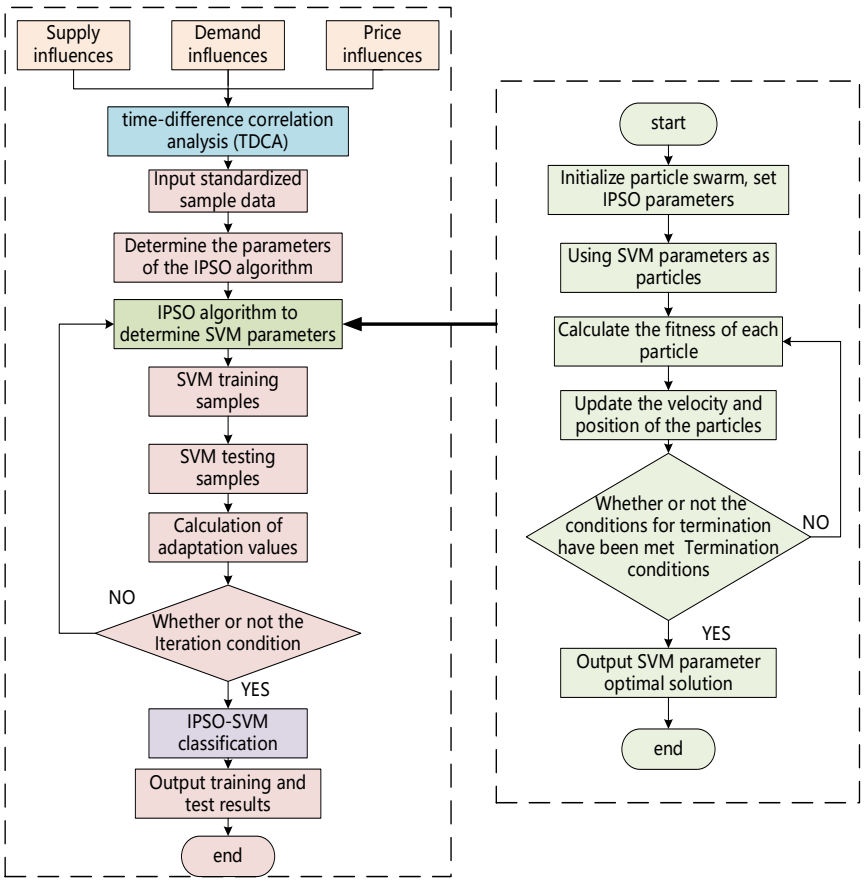

Figure 3. Flowchart of the IPSO-SVM-based early-warning model.

4.1. Improved particle swarm algorithm

In traditional particle swarm optimization (PSO), several key parameters—such as the inertia weight and learning factors—are typically fixed and manually specified. This lack of adaptability often leads to premature convergence, slow convergence speed, or entrapment in local optima, particularly when dealing with small-sample and nonlinear optimization problems. To overcome these limitations, this study proposes an improved particle swarm optimization (IPSO) algorithm by integrating three complementary adaptive strategies: inertia weight optimization, dynamic learning factor adjustment, and adaptive position update mechanisms.

(1) Optimization of the inertia factor ω. The inertia weight plays a key role in balancing global search capability and local search capability in particle swarm optimization. A smaller inertia weight tends to enhance the algorithm's local search ability, while a larger inertia weight tends to strengthen global search performance. To accommodate nonlinear problems that may possess multiple local extrema, which can render the search for a global optimum challenging, the exponential function's curvature is exploited to ensure that the inertia weight decreases as the number of iterations increases. This yields a fast-to-slow transition in the inertia weight, so that the overall algorithm emphasizes global exploration in the early stages and concentrates on local exploitation in the later stages, thereby facilitating faster convergence [41]. Consequently, the optimized inertia weight satisfies Equation (5):

$$\omega(t) = e^{-\frac{t}{t_{max}}} \tag{5}$$

Where t denotes the current iteration number, and t_{max} denotes the predetermined maximum number of iterations. Based on the formula, the inertia weight decreases as the number of iterations increases, thereby achieving a favorable balance between global search and local search capabilities.

(2) Optimization of learning factors c_1, c_2

The learning factor represents the individual particle's cognition and the swarm's cooperation. By optimizing these two factors, the global search capability and the local search capability can be enhanced from both the individual and the collective perspectives. Consequently, a logarithmic function is introduced to construct the nonlinearity and asynchrony of the learning factor, and this dynamic learning factor supplements the objectivity missing from a fixed value. The learning factor is allowed to take dynamic values for optimization, satisfying equations (6) and (7):

$$c_1 = c_{1\_max} - (c_{1\_max} - c_{1\_min}) \times ln(1 + (e-1) \times t/t_{max}) \tag{6}$$

$$c_2 = c_{2\_min} + (c_{2\_max} - c_{2\_min}) \times ln(1 + (e-1) \times t/t_{max}) \tag{7}$$

Among them, c_{1_max} and c_{2_max} are the upper limits of c_1 and c2, and c_{1_min} and c_{2_min} are the lower limits of c_1 and c2. This ensures that c_1 is controlled to take a larger value and c_2 to take a smaller value in the initial stage to enhance the global search capability, and c_1 to take a smaller value and c_2 to take a larger value in the final iteration to enhance the local search capability [42].

(3) Optimization of the position update formula

The position update equation of a particle determines its movement direction and step size in the search space, thereby directly influencing the algorithm's convergence and search efficiency. To address the limitations of fixed parameters in complex problems, adaptive parameters are introduced to adjust the convergence speed, improving the algorithm's flexibility and robustness. Dynamic parameter adaptation enables the algorithm to better accommodate the needs of different search phases: in the early iterations, the population convergence can be accelerated, while a fitness-order-based population selection mechanism can effectively suppress the diffusion of low-quality solutions; as iterations proceed, the parameter tuning strategy becomes progressively more conservative. By constraining the incremental velocity of particles, the population is kept within the convergence domain with an appropriate degree of dispersion, which helps prevent premature entrapment in local optima and also mitigates late-stage population divergence [43]. An adaptive parameter is incorporated to optimize, as shown in equations (8) and (9):

$$x_{id}(t) = x_{id}(t-1) + \eta \times v_{id}(t) \tag{8}$$

$$\eta = \frac{(\eta_{max} - \eta_{min})}{1 - exp\left[\alpha \times \left(t - \frac{t_{max}}{2}\right)\right]} + \eta_{min} \tag{9}$$

After t iterations, the position of the ith particle on dimension d is denoted as $x_{id}(t)$, which is updated in Eqs. (8) and (9) and is already adaptive. Here, η_{max} and η_{min} are the maximum and minimum values of the change, which are generally taken as $\eta_{max} \in [1.0,1.8]$, $\eta_{min} \in [0.4,0.8]$, and α is generally taken as $\alpha \in [0.005,0.015]$.

After t iterations, the velocity of the ith particle in dimension d is denoted as $v_{id}(t)$, which is calculated by:

$$v_{id}(t) = \omega v_{id}(t-1) + c_1 r_1(t)(x_{pbest_{id}} - x_{id}(t) + c_2 r_2(t))(x_{gbest_{id}} - x_{id}(t)) \tag{10}$$

Where ω is the nonnegative inertia factor, c_1 and c_2 are the nonnegative learning factors; r_1 and r_2 are the random numbers between [0,1]; $x_{pbest_{id}}$ is the individual optimal position; and $x_{gbest_{id}}$ is the global optimal position.

(4) Theoretical analysis of the proposed IPSO-SVM algorithm

To ensure the theoretical completeness and rigor of the proposed early-warning method, this subsection provides a formal analysis of the IPSO-SVM algorithm, focusing on the computational complexity of the integrated optimization process and the convergence characteristics introduced by the improved PSO strategy.

Theorem 1 (computational complexity of the IPSO-SVM algorithm):

Let N be the swarm size, D the dimensionality of the search space (i.e., the number of SVM parameters to optimize, typically $D = 2$ for (C, γ)), and T the maximum number of iterations. Let n denote the number of training samples, and K the number of folds in K-fold cross-validation used for fitness evaluation.

The overall time complexity of the IPSO-SVM algorithm is $O(T \cdot (N \cdot \mathcal{F} + N \cdot D))$, where $\mathcal{F}$ denotes the complexity of evaluating the fitness function for one particle.

Proof. The algorithm proceeds iteratively for T generations. In each iteration:

1) Velocity and position updates: For each of the N particles, updating its D-dimensional velocity (Eq. 10) and position (Eq. 8) involves $O(D)$ operations. This contributes $O(N \cdot D)$ per iteration.

2) Fitness evaluation (dominant cost): The fitness of a particle is defined as the K-fold cross-validation accuracy of an SVM model configured with the particle's position (C, γ). Training an SVM with a nonlinear kernel (e.g., RBF) on n samples typically represents a complexity between $O(n^2)$ and $O(n^3)$ in the worst case, depending on the optimization algorithm and dataset characteristics. Performing this K times per particle leads to a per-particle fitness evaluation cost of $O(K \cdot \mathcal{C}_{SVM}(n))$, where $\mathcal{C}_{SVM}(n)$ is the cost of a single SVM training. Therefore, the cost for all particles is $O(N \cdot K \cdot \mathcal{C}_{SVM}(n))$ per iteration.

Thus, the per-iteration complexity is $O(N \cdot D + N \cdot K \cdot \mathcal{C}_{SVM}(n))$. Since D is small and constant, and $K \cdot \mathcal{C}_{SVM}(n)$ is significantly larger, the dominant term is $O(N \cdot K \cdot \mathcal{C}_{SVM}(n))$. Over T iterations, the total complexity is $O(T \cdot N \cdot K \cdot \mathcal{C}_{SVM}(n))$. This analysis clarifies that the major computational burden stems from the repeated SVM training and validation during the PSO search, not merely from the PSO operations themselves. The improved PSO component (IPSO) itself retains the same asymptotic complexity $O(N \cdot D \cdot T)$ as standard PSO, but its enhanced convergence rate (established in Theorem 2) can reduce the required T to reach a satisfactory solution, thereby improving the effective computational efficiency of the overall IPSO-SVM workflow.

Theorem 2 (convergence acceleration of the IPSO-based optimization):

Consider the IPSO algorithm defined by Eqs. (5)–(10) for optimizing the parameters of an SVM. Under the conditions that:

i) The inertia weight $\omega(t) = e^{-t/t_{\max}}$ (Eq. 5) is a monotonically decreasing function mapping from $(0,1]$ to $(0,1]$.

ii) The cognitive and social learning factors $c_1(t), c_2(t)$ (Eqs. 6, 7) are bounded, asynchronous, and satisfy $c_1(t)$ decreasing while $c_2(t)$ increasing with t.

iii) The adaptive position update parameter $\eta(t)$ (Eq. 9) is bounded, then the particle velocity variance decays more rapidly compared to the standard PSO with fixed parameters. This structured adaptive parameter control promotes a faster transition from global exploration to local exploitation, leading to accelerated convergence in probability toward a stable equilibrium region of the parameter search space.

Proof. The convergence of PSO and its variants has been extensively studied through dynamic system theory and stochastic analysis. The standard PSO with fixed parameters can be modeled as a stochastic linear dynamic system. Its convergence condition and rate are influenced by the eigenvalues of its iteration matrix, which depend on $\omega, c_1,$ and c_2.

The proposed improvements directly target these parameters to enhance convergence:

1) Exponentially decaying inertia weight $\omega(t)$: Starting from a value close to 1 enhances global exploration. Its monotonic decay to near zero ensures the system's spectral radius contracts over time, forcing the swarm to shift focus from exploration to exploitation. This decay schedule is more aggressive than typical linear decreases, promoting faster stabilization.

2) Asynchronous logarithmic learning factors $c_1(t), c_2(t)$: Initially, a high c_1 and low c_2 emphasize individual particle memory (exploration). The complementary logarithmic adjustment causes c_1 to decrease and c_2 to increase, gradually shifting emphasis to swarm social learning (exploitation). This asynchronous guidance provides a more refined search trajectory than fixed or synchronously changing factors.

3) Adaptive position update $\eta(t)$: This sigmoidal adjustment moderates the particle step size, helping to prevent oscillation in early stages and excessive conservatism in later stages, further stabilizing convergence.

Collectively, these adaptive mechanisms ensure that the expected particle trajectory follows a search path that reduces the fitness function (cross-validation error) more efficiently. Formally, they lead to a faster reduction in the swarm's collective fitness variance $\mathrm{Var}(f(X_i(t)))$. In the context of optimizing the SVM's hyperparameter response surface, this translates to the IPSO algorithm locating a near-optimal (C, γ) pair within fewer iterations ($T' < T$) compared to the standard PSO, for a given desired fitness threshold. Consequently, the IPSO-SVM model training benefits from this accelerated parameter search, achieving the claimed enhancement in "convergence speed and performance" as stated in the introduction.

These two theorems provide the formal foundation supporting the second major contribution of this work. Theorem 1 accurately captures the full computational cost of the hybrid algorithm, while Theorem 2 explains how the proposed improvements to PSO mechanistically lead to faster convergence during the SVM parameter optimization phase. This theoretical analysis confirms that the major contribution—using an improved PSO to search for optimal SVM parameters—is well-founded: it enhances convergence, which, in turn, improves training performance by reducing computational cost, exactly as claimed in the introduction.

4.2. Constructing IPSO-SVM-based early-warning models

In this paper, an improved particle swarm algorithm is used to optimize the parameters and penalty factors of the kernel function of the support vector machine, to construct a prediction model for the early-warning level of silicon supply and demand. The support vector machine prediction model can solve the nonlinear optimization problem [44]. The functional expression of the SVM model is shown in Equation (11):

$$f(x) = \omega \times \varphi(x) + b \tag{11}$$

$$\begin{cases} \min \dfrac{1}{2}\|\omega\|^2 + c\sum_{i=1}^{N}\xi_i \\ s.t.\ \ y_i[\omega^T\varphi(x_i) + b] \geq 1 - \xi_i, \xi_i > 0 \end{cases} \tag{12}$$

Where ω denotes the normal vector of the hyperplane, c denotes the penalty parameter, ξ_i denotes the ith relaxation variable, b denotes the bias, N denotes the set of natural numbers, and x_i denotes the eigenvectors.

$$L(\omega, b, \xi, \alpha, \beta) = \frac{1}{2}||\omega||^2 + c\sum_{i=1}^{N}\xi_i - \sum_{i=1}^{N}\alpha_i[y_i(\omega^T\varphi(x_i) + b) - 1 + \xi_i] - \sum_{i=1}^{N}\beta_i\xi_i \quad (13)$$

Where $\alpha_i \geq 0$ and $\beta_i \geq 0$ are Lagrange multipliers. According to the Karush–Kuhn–Tucker (KKT) conditions, the solution to the original problem (10) can be obtained by solving the following dual problem:

$$\begin{cases} max \sum_{i=1}^{N}\alpha_i - \frac{1}{2}\sum_{i=1}^{N}\sum_{j=1}^{N}[\alpha_i y_i \varphi(x_i)^T \varphi(x_j)^T y_j \alpha_j] \\ s.t. \sum_{i=1}^{N}\alpha_i y_i = 0, 0 \leq \alpha_i \leq c \end{cases} \quad (14)$$

The relationship between the dual model (13) and the original model (11) is that the solution of (13) provides the optimal values of the Lagrange multipliers α_i, which are used to recover the hyperplane parameters of (11). Specifically, the normal vector is given by $\omega = \sum_{i=1}^{N}\alpha_i y_i \varphi(x_i)$, and the bias b can be computed from any support vector (with $0 < \alpha_i < c$) using $y_i(\omega^T\varphi(x_i) + b) = 1$.

In the context of classification prediction, the decision function for a new sample x is constructed as:

$$f(x) = sgn(\sum_{i=1}^{N}\alpha_i y_i K(x_i, x) + b) \quad (15)$$

Where $K(x_i, x) = \varphi(x_i)^T\varphi(x)$ is the kernel function. This function outputs the class label ($+1$ or -1) based on the sign of the expression, thereby performing classification. The Gaussian kernel function $K(x_i, x_j) = \exp(-\gamma \,||\, x_i - x_j \,||^2)$ is used in this study, where γ is a positive real parameter that controls the kernel width.

Regardless of which kernel function is used, the penalty factor c should be specified during training.

The core of applying the IPSO algorithm to optimize SVM parameters is to define a proper fitness function that accurately reflects the model's generalization performance. In this study, the goal is to find the optimal parameter pair (C, γ) that minimizes the classification error on unseen data. To avoid overfitting, the K-fold cross-validation accuracy is employed as the evaluation criterion. The fitness function is defined as the cross-validation error rate, and its exact mathematical expression is given by:

$$\text{Fitness}(\text{C}, \gamma) = 1 - （1/\text{K}） \sum_{k=1}^{k}\text{Accuracy\_k}(\text{C}, \gamma)(\text{X}) \quad (16)$$

where K is the number of cross-validation folds, and Accuracy k is the classification accuracy on the k-th validation fold.

Therefore, using the improved particle swarm algorithm to optimize the parameter γ and penalty factor c of the kernel function that needs to be specified in the support vector machine, the parameter γ and the penalty factor c are used as the particles. Specifically, each particle's position in the swarm is represented as a two-dimensional vector $\mathbf{x}_i = (c_i, \gamma_i)$, encoding a candidate solution for the SVM parameters. Initialize all the particles, i.e., assigning values to their velocities and positions, and setting

the individual's historically optimal pBest to the current position, and the optimal individual in the population is used as the current gBest; in each generation of evolution, the fitness of individual particles is computed function value. The fitness function, which guides the optimization process, is defined as the classification accuracy of the SVM model on the validation set using the parameters encoded by the particle. The PSO algorithm aims to maximize this fitness function and update pBest if the current fitness function value is better than the historical optimum and gBest if the current fitness function value is better than the global historical optimum [45].

5. Results

5.1. Data sources

The object of this paper is polysilicon; its upstream core supply is industrial silicon, and its direct downstream is silicon wafers. Sample data from January 2021 to November 2023 by Enterprise X, which is mainly engaged in polysilicon, are selected, including the rate of change in the order quantity of industrial silicon, the rate of change in the consumption quantity of industrial silicon, the rate of change in the price of silicon wafers, the rate of change in the price of polysilicon, and the rate of change in the price of substitutes. Data are targeted to the IPSO-SVM early-warning model; the input variables are the above five described, and the output variable is the warning level. From a total 139 data points, 70% are used as the training set and 30% as the test set.

5.2. Data processing

In this paper, for uniform calculation, each influence factor and the ratio of supply and demand of silicon material will be converted into the form of rate of change P_i uniformly by the conversion formula

$$P_i = \frac{V_i - V_{i-1}}{V_i} \tag{17}$$

Where V_i denotes the current period value, V_{i-1} denotes the previous period value, i denotes the period, and $i = 1,2,3,\ldots,n$ (n is the total number of periods).

The input variables are processed using the normalization formula

$$x_i^* = \frac{x_i - x_{min}}{x_{max} - x_{min}} \tag{18}$$

x_i^* denotes the normalized value, x_i denotes the original value, x_{min} denotes the minimum value in the data sample, and x_{max} denotes the maximum value in the data sample.

5.3. Selection of early-warning indicators

(1) Calculate the time-difference correlation coefficient

The data cover three factors affecting the historical polysilicon supply/demand ratio: the supply side, the demand side, and overall supply/demand. These include the rate of change of industrial silicon price, industrial silicon order quantity, and industrial silicon consumption. They also include the rate of change of wafer price, the price of substitutes, and the price of polysilicon. The time-difference correlation coefficients between these factors and the change in the polysilicon supply/demand ratio is calculated, and the results are shown in Table 3.

Table 3. Correlation coefficients of the time difference of each influencing factor.

Sources	Factor	Pilot phase	Correlation coefficient of time difference
Supply side	Rate of change in order quantities of industrial silicon	-3	0.494868879
	Rate of change in industrial silicon consumption	-3	0.554879683
	Rate of change in industrial silicon prices	-3	0.010623955
Demand side	Wafer price change	-3	0.210333824
	Rate of change in price of alternatives	-1	0.29871925
Supply and demand	Rate of change in polysilicon prices	-1	0.390013653

The polysilicon supply/demand ratio change rate is employed as the benchmark indicator. Using sample data from January 2021 to December 2023, the correlation coefficients of the time differences for each alarm indicator are computed. Given that weekly or semi-monthly polysilicon price movements exhibit limited short-term fluctuation, the calculations are performed on a monthly basis. Acknowledging that polysilicon prices may fluctuate within a monthly period and that price and market dynamics influence each other, thereby affecting changes in the polysilicon supply/demand ratio within the enterprise, an excessively short lead time may omit the optimal lead time, while an excessively long lead time may yield unreliable results. Consequently, pilot lead times of 1, 2, and 3 months are considered, and the time-difference correlation coefficient with the largest absolute value is selected.

(2) Screening for warning indicators

First, according to the general classification based on the correlation coefficient, very weak or no correlations are excluded so that the correlation coefficient is in the [0.0,0.2) of the influencing factors. Therefore, industrial silicon price change rate is excluded. Then, polysilicon supply/demand warning indicators are identified as the rate of change of industrial silicon orders J1, the rate of change of industrial silicon consumption J2, the rate of change of silicon wafer prices J3, polysilicon price changes J4, and the rate of change of substitution prices J5 (hereinafter, for ease of expression, in the form of J_i for the various warning indicators). The correlation between the warning indicators and the supply/demand ratio is generally moderately weak and weakly correlated, reflecting the complexity of the changes in internal and external supply and demand for polysilicon. Therefore, it is not appropriate to use a single indicator for early-warning studies.

Second, gray correlation analysis is used to verify whether the connection between each alarm indicator and the benchmark indicator (polysilicon supply/demand ratio) is close; the size of the gray correlation value can also intuitively reflect the degree of correlation between the two [46]. Calculated results from high to low are as follows: J3 is 0.959, J1 is 0.9, J5 is 0.893, J2 is 0.873, and J4 is 0.75. It can be seen that the gray correlation of all the indicators is greater than 0.85 (except for polysilicon prices), indicating that the correlation between the indicators is stronger; as such, indicators are selected using the principles of science, representativeness, and relevance.

5.4. Determination of early-warning levels

(1) Determination of the level of warning indicators

The volatility of the domestic macro market is used as a reference, i.e., the volatility of the supply/demand ratio of polysilicon owned by enterprises is considered based on the volatility of the domestic polysilicon supply/demand ratio. Figure 4 shows the fluctuation of the domestic polysilicon supply/demand ratio from 2021 to 2023 (the polysilicon supply side is quantified by polysilicon production and the demand side by polysilicon consumption by silicon wafers, which are directly downstream of polysilicon).

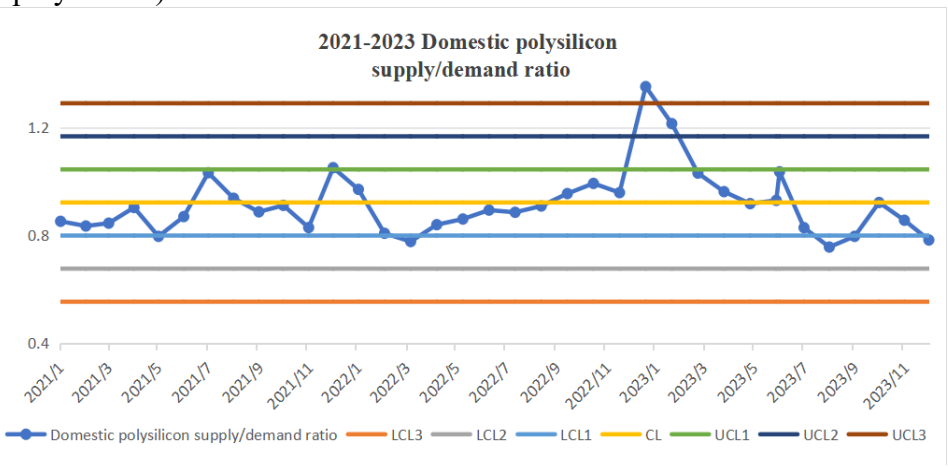

Figure 4. Fluctuations in the rate of change of domestic polysilicon supply/demand ratio.

By organizing the relevant data and using the Six Sigma principle form, i.e., $(-\infty, \mu-3\sigma),[\mu-3\sigma, \mu-2\sigma),[\mu-2\sigma, \mu-\sigma)[\mu-\sigma, \mu+\sigma)[\mu+\sigma, \mu+2\sigma)[\mu+2\sigma, \mu+3\sigma)[\mu+3\sigma, +\infty)$ to plot the preliminary $\mu \pm 3\sigma$ form of the fluctuation of the domestic polysilicon supply/demand ratio from January 2021 to December 2023 (Figure 4), it can be seen that from the 36 pieces of data, 4 are located in the $[\mu-2\sigma, \mu-\sigma)$ and $[\mu+\sigma, \mu+2\sigma)$ interval, 1 is located in $[\mu+2\sigma, \mu+3\sigma)$, and 1 is located in $[\mu+3\sigma, +\infty)$. Using the domestic market volatility as a criterion and combining it with the historical market volatility, 70% of the volatility is considered normal, 15% is considered third-level warning, 10% is considered second-level warning, and 5% is considered first-level warning. This probability is used to find the corresponding σ value against the σ level table:

Table 4. Classification of warning levels and thresholds for warning indicators.

Warning level	J1	J2	J3	J4	J5
1	(-∞, -0.453)	(-∞, -0.310)	(-∞, -0.178)	(-∞, -0.284)	[-∞, -0.227)
2	[-0.453, -0.268)	[-0.310, -0.190)	[-0.178, -0.113)	[-0.284, -0.176)	[-0.227, -0.150)
3	[-0.268, -0.114)	[-0.190, -0.090)	[-0.113, -0.058)	[-0.176, -0.087)	[-0.150, -0.074)
4	[-0.114, 0.204]	[-0.090, 0.116]	[-0.058, 0.055]	[-0.087, 0.098]	[-0.074,0.079]
5	(0.204, 0.359]	(0.116, 0.217]	(0.055, 0.110]	(0.098, 0.187]	(0.079,0.156]
6	(0.359, 0.543]	(0.217, 0.336]	(0.110,0.175]	(0.187, 0.294]	(0.156,0.233]
7	(0.543, +∞)	(0.336, +∞)	(0.175, +∞)	(0.294, +∞)	(0.233, +∞]

Derivation: Normal state: $[\mu - 0.525\sigma, \mu + 0.525\sigma]$, positive level 3 alert $(\mu + 0.525\sigma, \mu + 1.035\sigma]$, negative level 3 alert $[\mu - 1.035\sigma, \mu - 0.525\sigma)$, positive level 2 alert $(\mu + 1.035\sigma, \mu + 1.645\sigma]$, negative level 2 alert $[\mu - 1.645\sigma，\ \mu - 1.035\sigma)$, positive level 1 alert $(\mu + 1.645\sigma, +\infty]$, negative level 1 alert $(-\infty, \mu - 1.645\sigma)$. Since this fluctuation is the result of the joint effect of the warning indicators, the fluctuation interval of each warning indicator is divided according to this standard. According to this standard, the mean and standard deviation of each warning indicator of the raw data are calculated, and the determined warning degree and corresponding warning limit of each indicator are shown in Table 4.

(2) Determination of baseline indicator levels

The weights of the time-difference correlation coefficients of each warning indicator with the benchmark indicator (polysilicon supply/demand ratio) are calculated every month ω_i, the weights of the time-difference correlation coefficients of each warning indicator are divided by 0.254 for J1, 0.285 for J2, 0.108 for J3, 0.200 for J4, and 0.153 for J5, and the total cumulative weights are 1.

For the different warning levels of the indicators, scores are assigned as follows: Levels are negative third warning, negative second warning, negative first warning, normal state, positive first warning, positive second warning, and positive third warning. These levels correspond to scores of 1, 2, 3, 4, 5, 6, and 7, respectively. Set the baseline of the early-warning index (generally for the normal state of the warning index, set to 100), and calculate the historical moment of each period of the warning index. Of the early-warning index, set to 100, calculate the early-warning index for each period of the historical moment Zj. Based on the calculated mean and standard deviation of the warning index, the warning levels and corresponding thresholds are determined. For each period, the warning index is computed using the time-difference correlation coefficient and the rate of change of the silicon supply/demand ratio. The resulting thresholds for each warning level are negative first-level (25, 69.5675), negative second-class warning [69.5675,80.8525), negative second-class warning [69.5675, 80.8525], negative second-class warning [69.5675, 80.8525, 80.8525, 80.8525], warning index for the period 80.8525), negative third level of warning (80.8525,90.2875), normal status [90.2857,109.7125]; positive third level of warning (109.7125,119.1475], positive second level of warning (119.1475,130.4325], and positive first level of warning (130.4325,175).

Table 5. Sample data.

J1	J2	J3	J4	J5	Warning level
0.038952537	-0.290697674	0.114490161	0.1796875	0.047008547	5
-0.015185885	0.237704918	-0.051364366	0.324503311	0.043877551	3
0.019067119	0.029801325	-0.115623237	0.05	0.06744868	4
-0.03409305	0.282958199	0.116709184	-0.023809524	0.27032967	4
-0.072087884	-0.363408521	0.059394632	0.009756098	0.193771626	4
-0.083992995	0.078740157	-0.044743935	0.125603865	0.262681159	4
-0.580682166	0.138686131	0.10214447	0.145922747	0.182209469	5
-0.638883823	-0.125	-0.086021505	0.011235955	-0.004854369	4
0.388383838	-0.043956044	0.154061625	-0.148148148	-0.008536585	4
0.168483647	-0.005649718	0.085113598	0.020833333	0.244131455	7
...	...	...	...	...	...
0.782837504	0.046477351	0.088328076	-0.01210858	0.280284791	4

The warning indicators for each period in the final calculated data results are used as input variables to the prediction and warning model, and the warning degree is used as the output of the prediction and warning model. The sample data for the prediction model based on the improved PSO-optimized support vector machine are shown in Table 5.

5.5. Parameterization of IPSO-SVM model and evaluation indexes

Table 6. Model parameter settings.

Parameters	Description	Numerical value
c1	PSO parameter local search capability	1
c2	PSO parameter global search capability	1
maxgen	Maximum number of evolutions	60
sizepop	Maximum population size	15
wV	Elasticity coefficient for velocity in the rate update equation	[0.8,1.2]
wP	Elasticity coefficient for velocity in the population renewal equation	[0.8,1.2]
popcmax	Maximum value of the variation of the SVM parameter c	10^2
popcmin	Minimum value of the variation of the SVM parameter c	10^{-1}

This paper uses different prediction models together with the method proposed here for comparative experimental analysis. Parameter settings for the proposed method of silicon supply/demand prediction are shown in Table 6.

To validate the performance of the model, the prediction of silicon supply/demand warning levels is evaluated. In addition to using the basic classification evaluation metric, accuracy, the warning model also involves multi-category alert levels. To assess the overall performance of the classification model across all categories, macro or micro average metrics are necessary. Since sample data are unevenly distributed across alert categories, micro average is used. Accuracy is calculated using the following formula:

$$Accuracy = \frac{TP + TN}{TP + TN + FP + FN} \tag{19}$$

where TP denotes the true class, TN denotes the true-negative class, FP denotes the false-negative class, and FN is the false-positive class. Micro average is calculated as follows, where t_j denotes the number of samples predicted by the model to be in class j and belonging to class j, x_j denotes the number of samples predicted by the model to be in class j, and y_j denotes the number of samples that belong to class j:

$$P_{micro} = \frac{\sum_{j=1}^{k} t_j}{\sum_{j=1}^{k} x_j} \tag{20}$$

$$R_{micro} = \frac{\sum_{j=1}^{k} t_j}{\sum_{j=1}^{k} y_j} \tag{21}$$

$$F_{1_{micro}} = \frac{2}{\frac{1}{P_{micro}} + \frac{1}{R_{micro}}} \tag{22}$$

5.6. Analysis of results

To verify the superiority of the silicon supply and demand early-warning model proposed in this paper, a dataset is used to set up comparison experiments between different models. First, the proposed IPSO-SVM model is compared with the base model SVM, the general optimization model PSO-SVM, and another algorithmic optimization model, GWO-SVM. As the base model for classification, the SVM and PSO-SVM models perform better on large sample data when the parameters are appropriately selected. The GWO-SVM model, as a newer algorithm optimizing support vector machines, can find the optimal parameter values faster and more accurately. Second, the IPSO-SVM model is compared with the PSO-SVM model. The improvement of the IPSO-SVM involves updating the position formulas for the inertia factor, learning factor, and particles. In other words, the particle swarm algorithm is enhanced by applying a combination of strategies. This approach differs from the WPSO-SVM model, which only adapts the inertia factor, from the CPSO-SVM model, which only dynamizes the learning factor, and from the XPSO-SVM model, which only optimizes the particle position update formula. Comparison and analysis of the supply and demand warning model proposed in this paper proves its superiority in classification ability of alertness.

(1) Comparative analysis of models

Table 7 presents the evaluation results of the classification performance for different models in the context of vigilance level prediction. The traditional SVM model performs poorly on the small-sample dataset used in this study, primarily due to its decision boundary definition, which easily leads to overfitting. In comparison, the method proposed in this paper achieves a balance between model complexity and overfitting prevention by adaptively adjusting the penalty parameter C in SVM, resulting in a 26.69% improvement in accuracy. The PSO-SVM model exhibits slow convergence, largely influenced by the small-sample data characteristics, which cause fluctuations in the model's loss value. Setting the learning rate too high may prevent the model from converging. By introducing adaptive parameter settings for the learning factors, the proposed method improves accuracy by 5.63%. Furthermore, compared with the gray wolf optimizer-optimized SVM (GWO-SVM)—a metaheuristic algorithm that mimics the leadership hierarchy and hunting behavior of gray wolves to search for optimal SVM parameters—the proposed method also achieves a 5.63% increase in accuracy. When the number of samples in certain categories is significantly smaller than in others, classifiers tend to exhibit bias, leading to reduced accuracy in minority classes. While PSO-SVM and GWO-SVM perform well in majority classes, they lack focus on minority categories. In summary, the IPSO-SVM model proposed here demonstrates clear advantages in classifying silicon supply/demand warning levels. It not only outperforms traditional SVM and other metaheuristic-optimized SVM models but also effectively handles class imbalance by accounting for categories with different sample proportions.

Table 7. Comparative analysis of different models.

Models	Indicators	Numerical value
SVM	Accuracy	71.0526%
	$F_{1_{micro}}$	83.077%
PSO-SVM	Accuracy	92.1052%
	$F_{1_{micro}}$	93.333%
GWO-SVM	Accuracy	92.1052%
	$F_{1_{micro}}$	93.333%
IPSO-SVM	Accuracy	97.3684%
	$F_{1_{micro}}$	97.368%

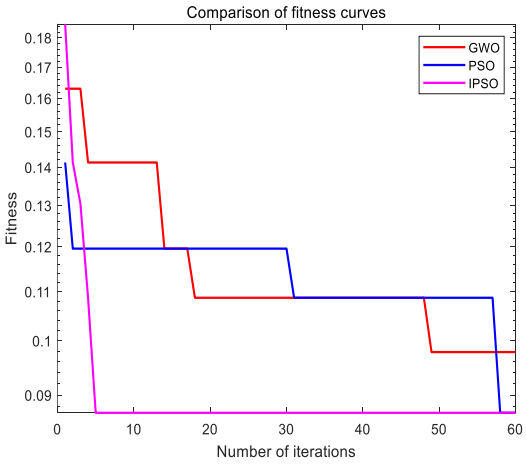

Figure 5. Model comparison fitness curves.

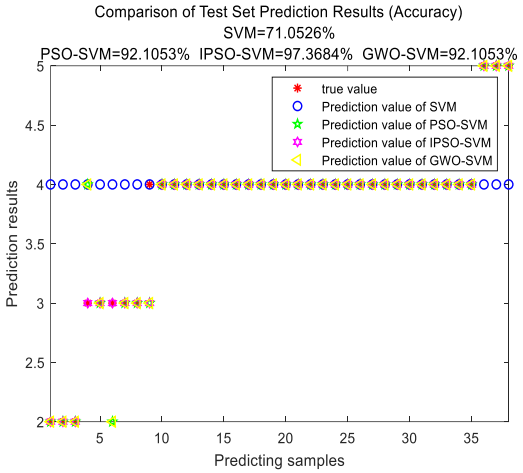

Figure 6. Test set prediction results.

The fitness curves in Figure 5 quantitatively demonstrate the superior convergence of IPSO, which reaches the lowest fitness value (approximately 0.095) in the fewest iterations, outperforming both PSO and GWO. As shown in Figure 6, the IPSO-SVM model achieves the highest test accuracy of 97.37%, a significant improvement over SVM (71.05%), PSO-SVM (92.11%), and GWO-SVM (92.11%). A numerical analysis of the confusion matrices in Figure 7 confirms the robustness of IPSO-SVM. It achieves perfect classification (100% precision and recall) for Class 3 and 5, and the highest recall (96.3%) for the key Class 4, demonstrating balanced performance across all warning levels.

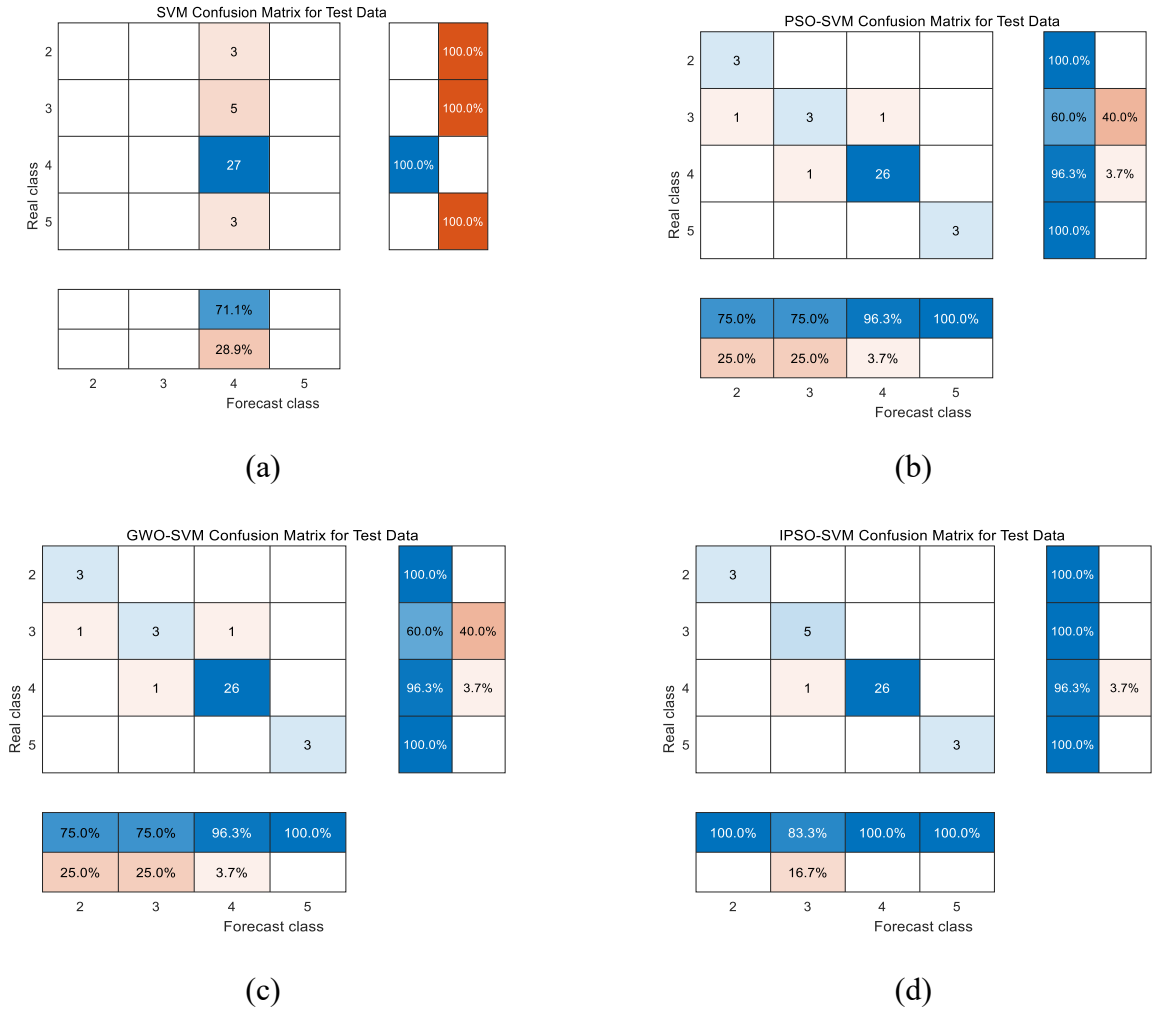

Figure 7. Confusion matrix optimized by different algorithms. (a) SVM model. (b) PSO-SVM model. (c) GWO-SVM model. (d) IPSO-SVM model.

(2) Comparative analysis of improvement strategies

Table 8 presents the IPSO-SVM model. Compared with single-strategy improved particle swarm algorithms, IPSO-SVM shows better performance. For example, the WPSO-SVM model, which only makes the inertia factor dynamic, has improved ability to solve nonlinear problems to some extent. However, its global search ability and local development ability remain unbalanced. The CPSO-SVM model, which only dynamizes the learning factor, balances global and local search abilities in the early stage. However, the inertia factor remains subjective and cannot adapt to changes in the algorithm's population. The XPSO-SVM model, which only improves the particle position updating formula, helps prevent particle dispersion in the late stage of optimization to some extent. Nevertheless, it does not enhance the ability to search for the optimal solution. In this paper, the method improves the updating formulas of the inertia factor, learning factor, and particle position. At the same time, it enhances the algorithm's search capability and dynamic adaptability to population size. As a result, the PSO algorithm achieves a better balance between global search ability and local development when searching for the optimal values of the SVM model. This enhanced balance is crucial for an early-warning system, as it ensures the model can reliably identify complex, nonlinear patterns indicative of impending supply/demand imbalances. In the alert classification prediction of silicon supply/demand

warning, the accuracy is improved by 3.5091% on average compared with other single-strategy optimization models. This significant improvement in classification accuracy directly translates to more precise and reliable warnings, fulfilling the core requirement of an effective early-warning system to minimize both false alarms and missed detections. The IPSO-SVM model proposed in this paper obtains higher accuracy performance for the alert classification prediction of silicon material supply and demand warning in the comparison of improved strategies.

Table 8. Comparative analysis of improvement strategies.

Models	Indicators	Numerical value
IPSO-SVM	Accuracy	92.1053%
	$F_{1_{micro}}$	93.333%
WPSO-SVM	Accuracy	86.8412%
	$F_{1_{micro}}$	88.0%
CPSO-SVM	Accuracy	89.4737%
	$F_{1_{micro}}$	89.473%
XPSO-SVM	Accuracy	89.4737%
	$F_{1_{micro}}$	89.473%

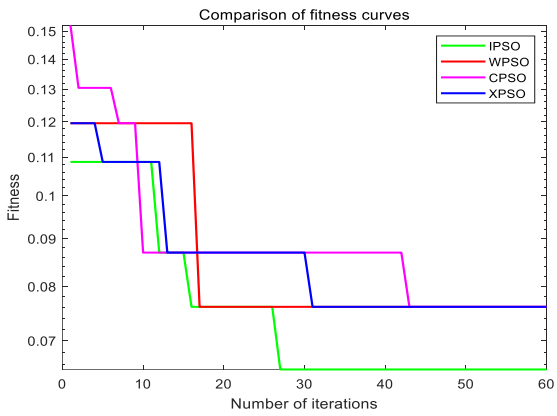

Figure 8. Optimization strategy fitness curve.

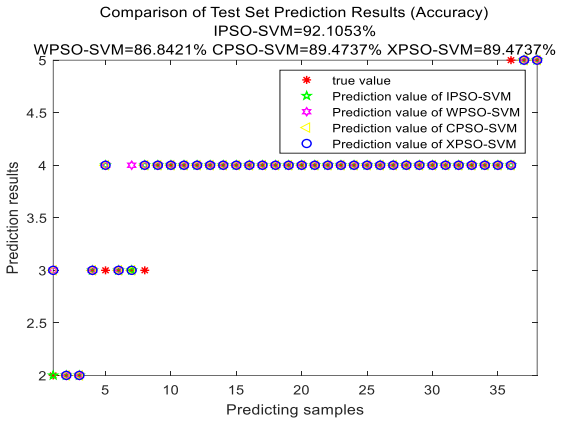

Figure 9. Test set prediction results.

To further validate and visualize the classification performance of the proposed method for silicon supply/demand alertness, the polysilicon supply/demand dataset is analyzed. The experimental training set and test set are visualized, as shown in Figures 6 and 9. These figures compare and analyze the classification predictions of the proposed method with those of other models. The predicted value of the IPSO-SVM represents the classification result of this study's method, while the results of the other models represent the comparative classification outcomes. The true value indicates the actual alertness level of the silicon supply/demand situation. As shown in the confusion matrices (Figures 7 and 10), the proposed model demonstrates strong adaptability to small-sample data. It achieves

superior performance on imbalanced classifications by accurately recognizing both majority and minority categories. The IPSO-SVM model proposed in this paper presents a better classification effect on the alertness and can classify the most real values into the right categories. In the fitness curves of the algorithm (Figures 5 and 8), the proposed IPSO-SVM performs better than other models. Compared with the traditional classification model SVM and with GWO-SVM and PSO-SVM, IPSO-SVM shows clear advantages. It also outperforms WPSO-SVM, CPSO-SVM, and other models that only improve a single parameter. The IPSO-SVM algorithm balances the global search ability and local development ability of PSO through inertia weights, learning rate, and particle updating speed. As a result, the fitness curves of IPSO converge more smoothly. The convergence speed is faster, and the algorithm can more accurately find the optimal values of SVM's parameters. Overall, this leads to a comprehensive improvement in classification accuracy.

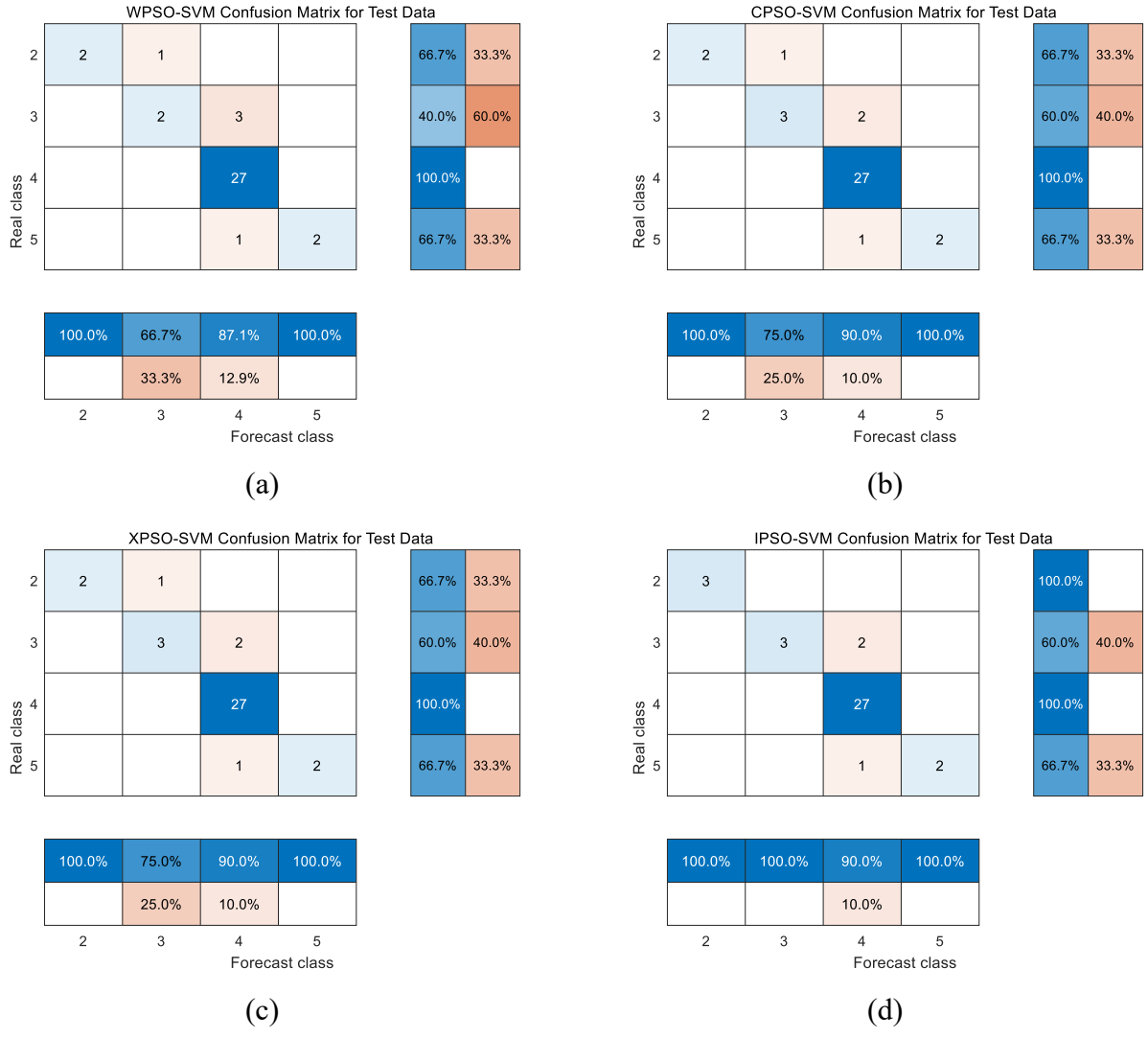

Figure 10. Confusion matrix improved by different strategies: (a) WPSO-SVM model; (b) CPSO-SVM model; (c)XPSO-SVM model; and (d) IPSO-SVM model.

(3) Analysis of ablation experiment

Table 9. Ablation study results of IPSO algorithm.

Group	ω	c1	C2	Position	Test accuracy (%)	Improvement (%)
1					73.68	0.00
2	√				92.11	18.43
3		√			86.84	13.16
4			√		86.84	13.16
5				√	89.47	15.79
6	√	√			94.11	20.43
7	√		√		94.11	20.43
8	√			√	94.74	21.06
9		√		√	91.25	17.57
10			√	√	91.25	17.57
11	√	√	√	√	97.37	23.69

To systematically evaluate the contribution of each component within the improved particle swarm optimization (IPSO) algorithm, a comprehensive ablation study was conducted. The results, summarized in Table 9, clearly delineate the performance impact of different component combinations.

The standard PSO (Group 1) established a baseline test accuracy of 73.68%. Each individual enhancement component demonstrably improved the algorithm's performance. The nonlinear inertia weight ω (Group 2) provided the most substantial individual boost, increasing accuracy by 18.43% to 92.11%. The asynchronous learning factors, c1 (Group 3) and c2 (Group 4), contributed identical improvements of 13.16%, while the adaptive position update strategy (Group 5) yielded a 15.79% gain. These results confirm that the nonlinear inertia weight plays the most critical role in balancing the algorithm's global exploration and local exploitation capabilities. Combination experiments further revealed significant synergistic effects among the strategies. Among the two-component combinations, the integration of ω with the adaptive position update (Group 8) achieved the best performance at 94.74% accuracy, representing a 21.06% improvement over the baseline. The three-component combinations also exhibited excellent performance. Ultimately, the full IPSO model (Group 11), integrating all proposed strategies, achieved the peak accuracy of 97.37%. This represents a 23.69% overall improvement over the standard PSO, unequivocally demonstrating strong positive synergy among all components.

In conclusion, the performance enhancement of the IPSO algorithm stems from the synergistic interaction of its components, with the nonlinear inertia weight being the most significant individual contributor. Each component enhances the algorithm's optimization performance and solution quality through distinct mechanisms. This study provides both a theoretical foundation and practical guidance for the advancement of PSO algorithms.

6. Conclusions

The supply and demand status of silicon materials in an enterprise is subject to fluctuations due to changes in the external supply chain market. From a supply chain perspective, numerous internal and external factors influence the internal balance of silicon supply and demand. However, there is currently a lack of early-warning mechanisms within enterprises to predict imbalances in silicon material supply and demand. To address this gap, this paper proposes an early-warning method for

silicon supply and demand based on IPSO-SVM from a supply chain perspective. Specifically, the method first analyzes factors affecting silicon supply and demand balance from three supply chain dimensions: upstream supply, downstream demand, and peer substitution. Time-difference correlation analysis is used to quantify the correlation between these factors and the silicon supply/demand ratio. Based on the correlation degree, five warning indicators are selected. Then, seven warning levels and corresponding thresholds are defined for these five indicators and one baseline indicator (the silicon supply/demand ratio), completing the model sample data preparation.

Next, a model based on IPSO-SVM is constructed. The particle swarm algorithm is first improved to overcome its disadvantages. The improved algorithm is then used to optimize the key parameters of the support vector machine, thereby enhancing classification accuracy. Finally, example data from enterprise X are introduced into the IPSO-SVM model and compared with other models. The results show that classification accuracy improves by 12.28% on average. Enterprises need to maintain the dynamic balance of supply and demand of silicon materials with the help of the supply chain under the fluctuation of the external market.

There are some limitations and potential future research directions. While this study identifies influencing factors from a macro supply chain perspective, actual enterprise operations also involve micro-level factors such as internal production capacity and energy storage. A future direction is to combine the characteristics of long capacity cycles and low-capacity elasticity of silicon materials to accurately match supply and demand across the entire supply chain. Additionally, the classification performance of the support vector machine model is affected by data with category imbalance. Therefore, the supply chain attributes of silicon materials can be further explored. The two approaches—prediction before warning and warning before prediction—can be combined to achieve dual warnings in both forward and reverse directions. Moreover, more advanced algorithms can be applied to improve the accuracy of early warnings.

Author contributions

Dudu Guo: Conceptualization, methodology, formal analysis, writing–original draft; Xue Zhang: Software, data curation, validation, visualization, writing–review & editing; Peifan Jiang: Resources, project administration, supervision, funding acquisition, writing–review & editing; Xiaojiang Zhang: Investigation, data curation, methodology, writing–original draft; Jinquan Zhang: Writing–review & editing, validation, visualization.

Use of Generative-AI tools declaration

The authors declare they have not used Artificial Intelligence (AI) tools in the creation of this article.

Acknowledgments

This research was supported in part by the Key R&D Program Project 2022B01015 of the Autonomous Region; Open Project Fund of National Engineering Center for Road Traffic Safety Control Technology (2024GCZKFKT05); General Project of Science and Technology Plan of the Ministry of Public Security (2024JSM04).

Conflict of interest

The research was conducted in the absence of any commercial or financial relationships that could be construed as a potential conflict of interest.

References

1. X. Hu, Overview of the development of solar photovoltaic power generation industry, *Shanghai Electr. Power*, **4** (2008), 365−370.
2. Q. Han, Brief description of the polysilicon market, *China Nonferrous Met,* **20** (2019), 42–43. https://doi.org/10.3969/j.issn.1673-3894.2019.20.030
3. T. Sun, Status and development trend of polysilicon industry in China under the background of carbon neutralization, *Mod. Chem. Res.,* **6** (2024), 185–187. https://doi.org/10.20087/j.cnki.1672-8114.2024.06.060
4. W. Hu, M. Lei, Z. Heng, Multi-prediction of electric load and photovoltaic solar power in grid-connected photovoltaic system using state transition method, *Appl. Energy*, **353** (2024), 122138.
5. Y. Feng, D. Gong, N. Gao, J. Zhang, Research on China's coal supply and demand monitoring system and prediction and early warning mechanism, *China Coal*, **48** (2022), 8–16. https://doi.org/10.3969/j.issn.1006-530X.2022.04.002
6. Y. Yang, C. Peng, Y. Yang, Y. Wang, Research on supply chain recovery strategy under disruption risk, *J. Syst. Simul.,* **33** (2021), 2771–2781. https://doi.org/10.16182/j.issn1004731x.joss.21-0825
7. L. Tao, H. Sun, Y. Cao, X. Wen, C. Liu, J. Yuan, Recovery strategies considering government subsidies in supply chain disruption scenarios, *Comput. Integr. Manuf. Syst.*, **28** (2022), 242–257. https://doi.org/10.13196/j.cims.2022.01.023
8. J. Wang, Y. Guo, Research on supply disruption contingency strategy considering product greenness, *Logist. Sci. Tech.,* **45** (2022), 1–6. https://doi.org/10.3969/j.issn.1002-3100.2022.06.002
9. H. Tang, F. Xia, D. Yang, F. Huang, X. Qiao, Early warning analysis of Oasis City development and water demand in arid areas–Take Urumqi City as an example, *Resour. Sci.,* **36** (2014), 1168–1174.
10. Q. Li, X. Chen, L. Wang, J. Wen, Study on the method of determining the early warning level of supply and demand of water resources in middle and short terms, *IOP Conf. Ser.: Earth Environ. Sci.,* **330** (2019), 032002. https://doi.org/10.1088/1755-1315/330/3/032002
11. Y. Zheng, J. Ma, Research on early warning ideas based on the association between short-term supply and demand differences and price fluctuations of agricultural products–Taking Beijing tomato market as an example, *Agric. Econ. Manag.,* **5** (2016), 81–89. https://doi.org/10.3969/j.issn.1674-9189.2016.05.009
12. H. Lu, T. Li, J. Lv, A. Wang, Q. Luo, M. Gao, et al., The fluctuation characteristics and periodic patterns of potato prices in China, *Sustainability*, **15** (2023), 7755. https://doi.org/10.3390/su15107755
13. W. Yang, B. Li, Prediction of grain supply and demand structural balance in China based on grey models, *Grey Syst.: Theory Appl.*, **11** (2021), 253–264. https://doi.org/10.1108/GS-09-2019-0039
14. J. Sun, Y. Lei, Analysis and early warning of supply and demand imbalance in China's rare earth market, *Resour. Sci.*, **41** (2019), 860–871. https://doi.org/10.18402/resci.2019.05.04

15. Y. Zhao, G. Lu, L. Zhao, Intelligent early warning and simulation of short-term wind power supply-demand equilibrium, *Comput. Simul.,* **39** (2022), 121–124.
16. Y. Li, P. Du, S. Li, M. Zhang, Research on energy demand intelligence and safeguard countermeasures in the context of peak carbon and carbon neutral patent early warning, *Manag. Technol. SME*, **11** (2021), 164–166.
17. S. An, F. An, X. Gao, A. Wang, Early warning of critical transitions in crude oil price, *Energy*, **280** (2023), 128089. https://doi.org/10.1016/j.energy.2023.128089
18. K. Zhou, Y. Chu, R. Hu, Energy supply-demand interaction model integrating uncertainty forecasting and peer-to-peer energy trading, *Energy*, **285** (2023), 129436. https://doi.org/10.1016/j.energy.2023.129436
19. X. Yao, S. Mao, Electric supply and demand forecasting using seasonal grey model based on PSO-SVR, *Grey Syst.: Theory Appl.*, **13** (2023), 141–171. https://doi.org/10.1108/GS-10-2021-0159
20. M. Pinhão, M. Fonseca, R. Covas, Electricity spot price forecast by modelling supply and demand curve, *Mathematics*, **10** (2022), 2012. https://doi.org/10.3390/math10122012
21. G. Lin, Y. Liang, A. Tavares, Design of an energy supply and demand forecasting system based on web crawler and a grey dynamic model, *Energies*, **16** (2023), 1431. https://doi.org/10.3390/en16031431
22. H. Song, J. Wang, G. Xu, Z. Tian, F. Xu, H. Deng, Novel model for pork supply prediction in China based on modified self-organizing migrating algorithm, *Agriculture*, **14** (2024), 1592. https://doi.org/10.3390/agriculture14091592
23. Y. Chen, Z. Xu, J. Wang, P. D. Lund, Y. Han, T. Cheng, Multi-objective optimization of an integrated energy system against energy, supply-demand matching and exergo-environmental cost over the whole life-cycle, *Energy Convers. Manag*., **254** (2022), 115203. https://doi.org/10.1016/j.enconman.2021.115203
24. Z. Shi, J. Li, X. Hu, Y. Zhang, Impact of natural disasters on supply and demand in China's grain market, *J. Catastrophol*, **38** (2023), 17–24. https://doi.org/10.3969/j.issn.1000-811X.2023.03.003
25. X. Zhao, S. Zhi, Analyzing and forecasting the security in supply-demand management of Chinese forestry enterprises by linear weighted method and artificial neural network, *Enterp. Inf. Syst.*, **15** (2020), 1280–1297. https://doi.org/10.1080/17517575.2020.1739343
26. H. Cai, S. Shen, Q. Lin, X. Li, H. Xiao, Predicting the energy consumption of residential buildings for regional electricity supply-side and demand-side management, *IEEE Access*, **7** (2019), 30386–30397. https://doi.org/10.1109/ACCESS.2019.2901257
27. Z. Li, F. Feng, A safety warning model based on IAHA-SVM for coal mine environment, *Sensors*, **23** (2023), 6614. https://doi.org/10.3390/s23146614
28. E. Bonah, X. Huang, R. Yi, J. H. Aheto, R. Osae, M. Golly, Electronic nose classification and differentiation of bacterial foodborne pathogens based on support vector machine optimized with particle swarm optimization algorithm, *J. Food Process Eng.*, **42** (2019), e13236. https://doi.org/10.1111/jfpe.13236
29. Y. Sun, J. Zhu, X. Yu, C. Ye, G. Fan, Research on early warning of power grid construction safety based on PSO-SVM model, *J. Phys.: Conf. Ser.*, **1449** (2020), 012037. https://doi.org/10.1088/1742-6596/1449/1/012037
30. Q. Song, M. Ma, W. Guo, T. Jiang, N. Pan, Health state diagnosis of air duct for photovoltaic inverter based on PSO-SVM classifier, *Microelectron. Reliab.*, **150** (2023), 115084. https://doi.org/10.1016/j.microrel.2023.115084

31. L. Tian, C. Shang, M. Li, Y. Wang, Research on classification of water stress state of plant electrical signals based on PSO-SVM, *IEEE Access*, **11** (2023), 125021–125032. https://doi.org/10.1109/ACCESS.2023.3330651
32. Y. Liang, S. Mao, M. Zheng, Q. Li, X. Li, J. Li, et al. Study on the prediction of low-index coal and gas outburst based on PSO-SVM, *Energies*, **16** (2023), 5990. https://doi.org/10.3390/en16165990
33. M. Li, D. Cheng, Z. Wang, Research on heating load prediction based on PCA-PSO-SVM, *Dist. Heat.*, **5** (2023), 146–153. https://doi.org/10.16641/j.cnki.cn11-3241/tk.2023.05.020
34. H. Ren, J. Zhang, Z. Ma, Optimized least squares support vector machine based on particle swarm algorithm for prediction of settlement of surrounding environment during foundation pit construction, *Value Eng.*, **43** (2024), 154–156. https://doi.org/10.3969/j.issn.1006-4311.2024.02.049
35. A. Qin, Q. Hu, Q. Zhang, Y. Lv, G. Sun, Application of sensitive dimensionless parameters and PSO-SVM for fault classification in rotating machinery, *Assem. Autom.*, **40** (2020), 175–187. https://doi.org/10.1108/AA-09-2018-0125
36. Y. Wei, Y. Li, M. Xu, W. Huang, Intelligent fault diagnosis of rotating machinery using ICD and generalized composite multi-scale fuzzy entropy, *IEEE Access*, **7** (2019), 38983–38995. https://doi.org/10.1109/ACCESS.2018.2876759
37. M. Li, Y. Li, N. Wu, T. Tian, T. Wang, Desert seismic random noise reduction framework based on improved PSO-SVM, *Acta Geod. Geophys.* **55**, (2020), 101–117. https://doi.org/10.1007/s40328-019-00283-3
38. C. Xu, L. Li, J. Li, C. Wen, Surface defects detection and identification of lithium battery pole piece based on multi-feature fusion and PSO-SVM, *IEEE Access*, **9** (2021), 85232–85239. https://doi.org/10.1109/ACCESS.2021.3067641
39. Y. Wang, X. Meng, L. Zhu, Cell group recognition method based on adaptive mutation PSO-SVM, *Cells,* **7** (2018), 135. https://doi.org/10.3390/cells7090135
40. Y. Yang, X. Han, J. Dai, X. Sun, Research on TBM boring speed prediction based on improved PSO-LSSVM, *Henan Sci.*, **40** (2022), 1642–1651. https://doi.org/10.3969/j.issn.1004-3918.2022.10.012
41. F. Xu, D. Zou, C. Li, H. Luo, M. Zhang, An improved particle swarm algorithm introducing Circle mapping and sine-cosine factor, *Comput. Eng. Appl.,* **59** (2023), 80–90. https://doi.org/10.3778/j.issn.1002-8331.2211-0290
42. Y. Xiao, Y. Zhao, Research on MPPT control strategy of improved particle swarm algorithm based on chaotic mapping and Gaussian perturbation, *J. Power Supply*, **23** (2025), 96–104. https://doi.org/10.13234/j.issn.2095-2805.2025.5.96
43. Y. Qin, L. Peng, Nonlinear inertial weight particle swarm algorithm with filtering mechanism, *Comput. Eng. Appl.*, **50** (2014), 35–38. https://doi.org/10.3778/j.issn.1002-8331.1208-0478
44. Y. Liu, H. Zhang, J. Xu, Y. Ren, J. Tang, Improved SVM regression model for PSO and its application in temperature prediction, *Comput. Syst. Appl.*, **32** (2023), 203–210. https://doi.org/10.15888/j.cnki.csa.009225
45. Q. Huang, H. Huang, Y. Zhang, X. Hu, Simulation prediction of tool wear based on multi-information fusion and improved PSO-SVM, *Res. Explor. Lab.*, **40** (2021), 119–123. https://doi.org/10.19927/j.cnki.syyt.2021.06.024

46. Y. Wang, X. Li, C. Yang, T. Yang, F. Lan, X. Tian, A dynamic Bayesian network risk assessment model for coal-fired power plants based on grey correlation and triangular fuzzy theory, *Comput. Stand. Interfaces*, **94** (2025), 104001. https://doi.org/10.1016/j.csi.2025.104001

AIMS Press